Green Chemistry

PAPER

View Article Online
View Journal | View Issue

Cite this: *Green Chem.*, 2024, **26**, 10152

Bioprocess development and scale-up for *cis,cis*-muconic acid production from glucose and xylose by *Pseudomonas putida*†

Sekgetho C. Mokwatlo, [a,b] Bruno C. Klein, [a,b] Pahola Thathiana Benavides,[b,c] Eric C. D. Tan, [a,b] Colin M. Kneucker,[a,b] Chen Ling,[a,b] Christine A. Singer,[a] Robert Lyons,[a] Violeta Sànchez i Nogué, [a] Kelley V. Hestmark,[a,b] Morgan A. Ingraham, [a] Kelsey J. Ramirez, [a] Christopher W. Johnson,[a,b] Gregg T. Beckham *[a,b] and Davinia Salvachúa *[a,b]

cis,cis-Muconic acid (MA) is a bio-based chemical that can be converted to direct replacement chemicals or performance-advantaged bioproducts. We recently engineered the bacterium *Pseudomonas putida* KT2440 for the co-utilization of glucose and xylose to produce MA. This study evaluates the effect of additional genetic modifications, media composition, and bioprocess strategy on MA titer, productivity, and yield in bioreactor cultivations. We achieve a MA titer of 47.2 g L^{-1}, a productivity of 0.49 g L^{-1} h^{-1}, and a yield of 0.50 C-mol C-mol^{-1} from glucose and xylose supplemented with 5% (v/v) corn steep liquor with a *P. putida* strain harboring the deletion of *gacS*. Additionally, we demonstrate efficient MA production from corn stover-derived sugars and scalability to 150 L bioreactors. Techno-economic analysis and life cycle assessment predict that adipic acid, derived from catalytic hydrogenation of MA, can achieve a selling price as low as $2.60 per kg, approaching cost parity and reducing greenhouse gas emissions by up to 80% relative to fossil carbon-based adipic acid.

Received 13th July 2024,
Accepted 28th August 2024

DOI: 10.1039/d4gc03424d

rsc.li/greenchem

Introduction

cis,cis-Muconic acid (MA) is a di-olefinic, C6-dicarboxylic acid that has garnered interest as a bio-based platform chemical. MA can be converted to multiple direct replacement chemicals such as adipic acid (AA), terephthalic acid, and caprolactam.[1–5] In addition, MA can be used directly or converted to new molecules, such as 3-hexenedioic acid, for the production of performance-advantaged bioproducts.[6–9] Biological production of MA was pioneered by Draths and Frost, who reported a *de novo* biosynthesis of MA from glucose *via* the shikimate pathway using engineered *Escherichia coli*.[1] Various hosts including *Corynebacterium glutamicum*[10] and *Pseudomonas putida* KT2440 (hereafter *P. putida*)[11,12] have also been engineered for MA production from glucose. Although glucose has been a common substrate in MA bioproduction studies, recent efforts with engineered strains of *E. coli*,[13] *P. putida*,[14] and *Saccharomyces cerevisiae*,[15] have achieved efficient glucose and xylose co-utilization, both abundant sugars in lignocellulose-derived hydrolysates.

P. putida is a genetically tractable, Gram-negative bacterium that has been used as a host to produce multiple bioproducts, including MA.[16,17] Previously, we demonstrated MA production in an engineered *P. putida* strain CJ200[12] (hereafter, CJ200 or the corresponding strain) from glucose, building on the work from Draths and Frost.[1] Briefly, glucose was converted to MA *via* the shikimate pathway by heterologous expression of genes encoding a 3-DHS dehydratase (*asbF*), protocatechuate decarboxylase (*aroY*), and its corresponding co-factor generating protein (*ecdB*),[18,19] and deletion of enzymes involved in the catabolism of MA and protocatechuate (*catRBC* and *pcaHG*, respectively). Additional genetic modifications to CJ200 increased yields from 0.064 to 0.33 (mol mol^{-1}), generating the strain CJ442.[20] However, CJ442 accumulated high concentrations of 2-ketogluconate in bioreactors, leading us to delete the glucose dehydrogenase gene *gcd* (strain CJ522, Table 1).[20] Although MA yields increased to 0.39 (mol mol^{-1}), *gcd* deletion caused growth deficiencies, which negatively impacted MA productivity.[20] To address this, we conducted adaptive laboratory evolution on glucose to identify beneficial mutations in isolated evolved strains, which highlighted that deletion of the transcriptional repressor gene *hexR* enables significantly

[a]*Renewable Resources and Enabling Sciences Center, National Renewable Energy Laboratory, Golden, CO, USA. E-mail: gregg.beckham@nrel.gov, davinia.salvachua@nrel.gov*
[b]*Agile BioFoundry, Emeryville, CA, USA*
[c]*Systems Assessment Center, Energy Systems and Infrastructure Analysis Division, Argonne National Laboratory, Lemont, IL, USA*

† Electronic supplementary information (ESI) available. See DOI: https://doi.org/10.1039/d4gc03424d

Table 1 Strains cited and used in this study

Strain	Genotype	References
CJ522	***P. putida* KT2440** ΔcatRBC::Ptac:catA ΔpcaHG::Ptac:aroY:ecdB:asbF ΔpykA::aroG-D146N:aroY:ecdB:asbF ΔpykF Δppc Δpgi-1 Δpgi-2 Δgcd	Johnson *et al.* (2019)[20]
GB062	**CJ522** Δ*hexR*	Bentley *et al.* (2020)[11]
GB271	**GB062** Δ*gacS* Δ*gntZ*	Bentley *et al.* (2020)[11]
LC224	**CJ522** ΔhexR ΔampC::PxylE*xylE:Ptac:xylAB:talB:tktA Δpgi-1::pgi-1 PP_1736-1737(intergenic)::Plac:ubiC-C22 xylE-A62V,A455V PPP_2569 G→A Δ*pykF*::P*tac:aroB*	Ling *et al.* (2022)[14]
KH083	**LC224** Δ*gacS*	This study
KH099	**LC224** Δ*gntZ*	This study

enhanced growth rates while maintaining MA yield at 0.35 (mol mol^{-1}) (strain GB62, Table 1).[11] Other identified mutations led us to test a double gene deletion (*gacS* and *gntZ*) in GB62 (strain GB271,[11] Table 1), which further improved MA productivity in bioreactors from 0.15 g L^{-1} h^{-1} in GB62 to 0.21 g L^{-1} h^{-1} in GB271.

Given the abundance of xylose in lignocellulosic hydrolysates, we recently incorporated the D-xylose isomerase pathway into GB62 (strain QP328),[14] and subjected this new strain to adaptive laboratory evolution and metabolic engineering.[14] Point mutations in the D-xylose:H$^+$ symporter gene (*xylE*), overexpression of *aroB* (which encodes the native 3-dehydroquinate synthase), and increased expression of a major facilitator superfamily transporter family (PP_2569) allowed MA production improvements from both sugars, achieving titers of 37 g L^{-1} at a productivity of 0.18 g L^{-1} h^{-1} and a yield of 0.46 (mol mol^{-1}) (strain LC224, Table 1).[14] However, LC224 did not incorporate the deletion of *gacS* or *gntZ*, and based on the observations from Bentley *et al.*,[11] we hypothesized that these genetic modifications could further enhance MA production metrics in LC224.

In this study, we sought to improve MA production from glucose and xylose through strain engineering, media optimization, and bioprocess development. Specifically, we evaluated the performance of *P. putida* LC224 with *gacS* or *gntZ* knocked out, and, with the optimal strain, we explored the effect of the bioprocess strategy, media composition, and scale. Lastly, we modeled a process to produce MA from lignocellulosic sugars and catalytic hydrogenation to produce AA, with techno-economic analysis (TEA) and life cycle assessment (LCA) to identify key drivers to enable further process improvements.

Results

Deletion of *gacS* in *P. putida* LC224 enhances MA production rates

Based on the MA productivity improvements observed in *P. putida* GB62 with *gacS* (PP_1650) and *gntZ* (PP_4043) deletions,[11] we first deleted these genes in strain LC224, generating strains KH083 and KH099, respectively (Table 1). These strains were evaluated and compared to LC224 in a plate reader using M9 medium with 5.4 g L^{-1} (30 mM) glucose and 2.3 g L^{-1} (15 mM) xylose, which is the ratio typically found in corn stover-derived hydrolysates.[21] Growth was monitored based on the optical density at 600 nm (OD_{600}). Deletion of *gacS* in KH083 reduced the growth lag by ~15 h compared to LC224 while KH099 showed a similar growth profile to LC224 (Fig. S1†). We next compared MA production in flasks by the three strains. KH083 exhibited the highest glucose utilization rate, followed by LC224 and KH099 (Fig. 1a–d), while xylose utilization was similar in all the strains. Both LC224 and KH083 achieved similar MA titers, yields, and productivities, which were higher than those observed in KH099 (Fig. 1a–d), suggesting that the deletion of *gntZ* is not beneficial in this genetic background.

We subsequently evaluated LC224 and KH083 in bioreactors using a batch mode cultivation strategy and modified M9 media supplemented with 50 g L^{-1} glucose and 25 g L^{-1} xylose. Both strains experienced longer lag phases (20 h) compared to the flask experiments, likely due to the higher initial sugar concentrations (Fig. 1e and f). Despite the longer lag phase, KH083 produced, on average, modestly higher MA titers, yields, and productivities than LC224 (Fig. 1e and f), up to 24.4 g L^{-1}, 0.47 C-mol C-mol^{-1}, and 0.34 g L^{-1} h^{-1}, demonstrating the benefit of the *gacS* deletion in LC224. Thus, we selected KH083 for further bioprocess development.

Initial sugar concentration and supplementation of corn steep liquor both impact KH083 performance in shake flasks

Based on the significantly longer growth lag observed in KH083 when cultivated at an initial total sugar concentration of 75 g L^{-1} compared to 7.65 g L^{-1} (Fig. 1b and f), we sought to understand the impact of initial sugar concentration on KH083, as this process parameter has important implications in bioprocess optimization (*i.e.*, higher initial sugar concentrations are preferred to mitigate product dilution). In addition, with the purpose of reducing the growth lag, we tested the effect of adding corn steep liquor (CSL) (10% v/v) to the cultivations. In the absence of CSL, we found that microbial growth was dependent on the initial sugar concentration. Namely, greater growth was achieved when starting with lower sugar concentrations at 30 h of incubation (the endpoint of this experiment) (Fig. 2a). CSL addition substantially decreased the lag time for all tested sugar concentrations to less than 2 h compared to media without CSL, except for 125 g L^{-1}, which exhibited a growth lag phase of 5 h. As a result, the overall glucose and xylose utilization at 30 h was also higher at low initial sugar concentrations, and this effect became less apparent when CSL was added in the media (Fig. 2b and c). Furthermore, based on the low sugar utilization at the beginning of the cultivations in the presence of CSL (Fig. S2†) but high growth rates, we hypothesize that the strain may utilize bio-available carbon from CSL prior to sugars. Regarding MA production, MA titers and productivities were consistently higher in the presence of CSL due to the enhanced sugar util-

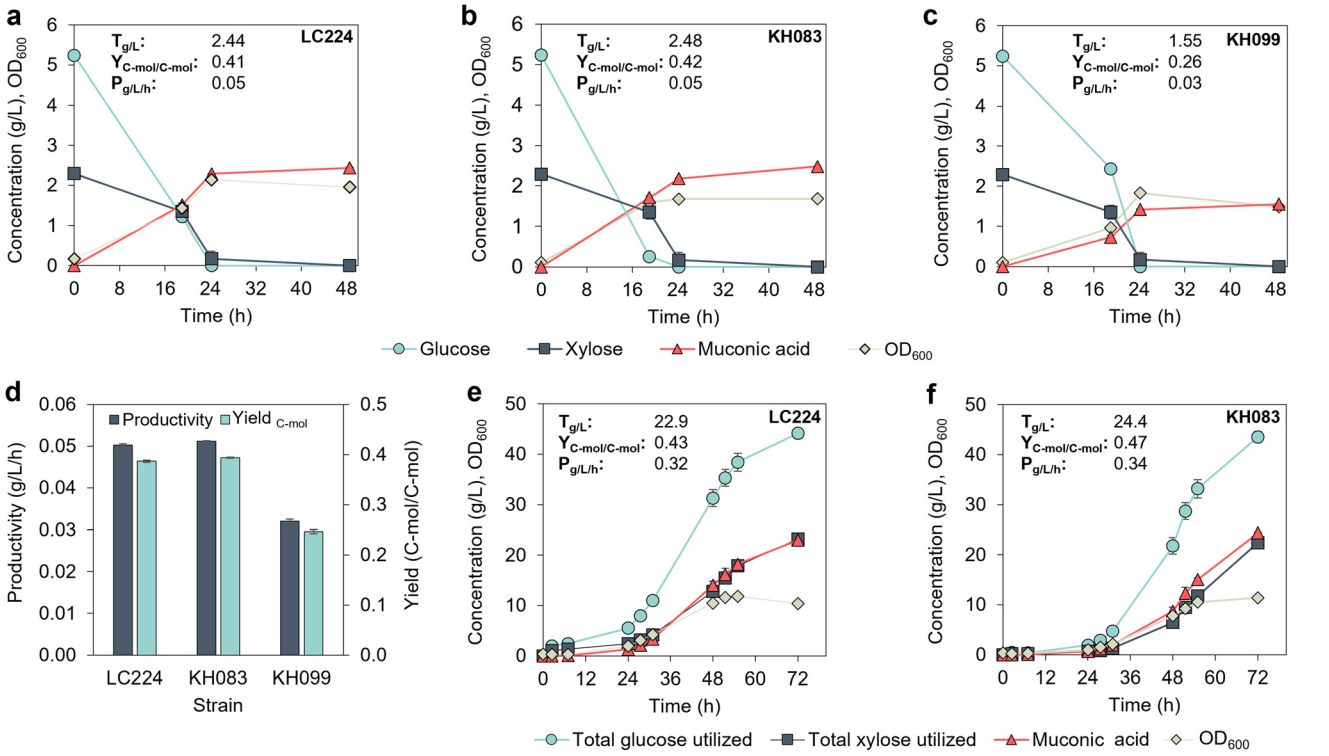

Fig. 1 Evaluation of *P. putida* strains in shake flasks and 0.5 L bioreactors. (a–c) Growth (OD_{600}), sugars, and MA profiles of strains KH083, LC224 and KH099 in shake flasks. pH was monitored and adjusted at every sampling point (targeting a range of pH 7 to 7.2). The data represent the average of three biological replicates, and the error bars represent the standard deviation. (d) Productivity and C-mol yield comparison for the strains in the shake flask experiments. (e and f) Growth (OD_{600}), sugars, and MA profiles of strains KH083 and LC224 in bioreactors using a batch cultivation strategy. Data show the average of biological duplicates, and the error bars represent the absolute error between duplicates. Titers (*T*), yields (*Y*), and productivities (*P*) are provided in the figure panels. Yield data are reported on a C-mol basis. Titers and productivities are calculated at the end time point. All data in this figure are provided in ESI 1.†

ization and decreased growth lags compared to minimal media (Fig. 2d and e). MA yield decreased with increasing initial sugar concentrations (Fig. 2f); however, sugar utilization was negligible in minimal media at 100 and 125 g L^{-1} sugar concentrations, limiting the ability to draw conclusions about those specific yields. Overall, these results demonstrate the benefits of using CSL to shorten growth lags and increase glucose and xylose utilization rates.

KH083 performance improves in bioreactor cultivations controlled at low sugar concentrations

The previous results suggest that microbial performance may not be significantly impacted if cultivations contain CSL and sugar concentrations lower than 100 g L^{-1}. To confirm this, we evaluated the effect of two cultivation strategies on MA production in 0.5 L bioreactors. The first strategy involved a batch phase initiated with a high sugar concentration (90 g L^{-1}), followed by a fed-batch phase with pulsed feeding to increase the sugar concentration above 50 g L^{-1} whenever it dropped below 20 g L^{-1} (Fig. 3a). The second strategy included a batch phase initiated at a low sugar concentration (15 g L^{-1}), with continuous feeding to maintain sugar concentrations between 5 and 25 g L^{-1} (Fig. 3b). Glucose and xylose feeding profiles and concentrations in the bioreactors are shown in Fig. S3.† Both the batch and fed-batch media contained 10% CSL (v/v).

KH083 exhibited superior performance in the cultivations maintained at low sugar concentrations, whereas high initial sugar concentration decreased growth and sugar utilization rates (Fig. 3a and b). The total sugar utilization after 24 h at low and high initial sugar concentrations was 49 g L^{-1} and 25 g L^{-1}, respectively, which resulted in higher MA productivity and titer in the former case (Fig. 3a–c). MA yield was also impacted by the starting sugar concentrations as evidenced by the molar yield reductions at high sugar concentrations (from 0.52 *vs.* 0.42 mol mol^{-1}) (Fig. 3d).

We hypothesized that bio-available components in CSL may be utilized by KH083. To understand the specific impact of CSL on performance metrics (*i.e.*, yield), we quantified the total organic carbon (TOC) content in CSL (TOC = 5.78 g L^{-1} in a 10% CSL solution on a volume basis). Then, we calculated the MA C-mol yield as the C-mol of MA produced divided by the C-mol utilized from glucose, xylose, and CSL, assuming full utilization of the TOC in CSL. Considering these calculations, MA yields from sugars are 0.50 and 0.40 C-mol $C\text{-mol}^{-1}$ at low and high initial sugar concentrations, respectively. Additionally, we also conducted a cultivation in a bioreactor containing CSL (5%,

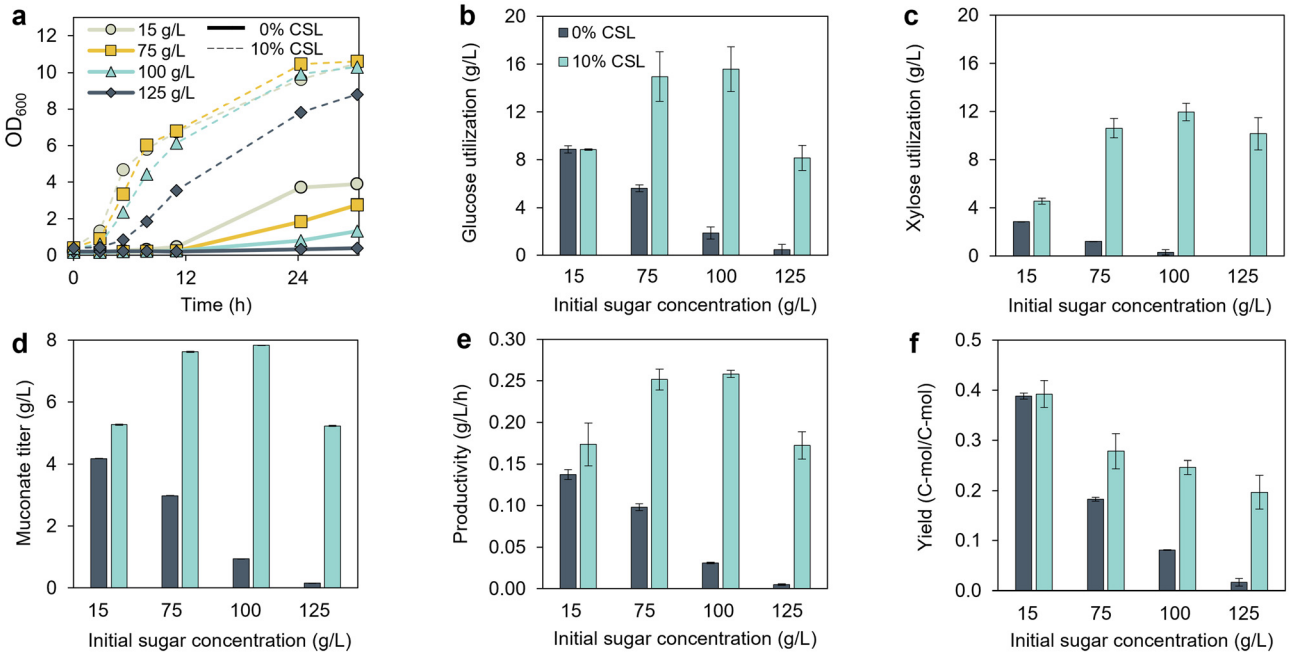

Fig. 2 Effect of initial sugar concentration and media composition on *P. putida* KH083 performance in shake flasks. (a) Bacterial growth (OD_{600}) over time, and (b) total glucose utilization, (c) total xylose utilization, (d) MA titers, (e) MA productivity, and (f) MA yield, all at 30 h of incubation and at different starting sugar concentrations (15, 75, 100 and 125 g L^{-1}) with and without supplementation of corn steep liquor (CSL) at 10% (v/v). Yield calculations do not account for C in CSL in this experiment. Glucose and xylose utilization profiles are shown in Fig. S2.† The glucose-to-xylose ratio was 2 : 1 (g/g). The data represent the averages of biological duplicates, and the error bars represent the absolute error between the duplicates. All data in this figure are provided in ESI 1.†

v/v) as the sole carbon source. A MA concentration of 0.43 g L^{-1} was produced from 2.89 g L^{-1} TOC in CSL (max OD_{600} of 4.34 after 6.7 hours), which confirms that MA can be produced from CSL. Accordingly, for accurate MA yield metrics from sugars, it is essential to consider the yields generated from CSL, which were factored into the subsequent experiments. Overall, this experiment indicated that maintaining low sugar concentrations in the bioreactors significantly improves KH083 bioprocess performance.

A CSL concentration of 5% (v/v) is optimal for MA production by KH083

To reduce the media costs, we investigated the effect of CSL concentrations lower than 10% (v/v) on MA production. Bioreactor cultivations were conducted in the optimal setup identified above, with an initial sugar concentration of 15 g L^{-1} and continuous fed-batch mode (Fig. S4†). CSL was added in both the batch and feeding media, at concentrations of 0, 1, 5% (v/v). As expected, based on the results obtained in flasks (Fig. 2a), KH083 displayed the lowest growth rates in the absence of CSL (Fig. 4a). Indeed, growth lags were not observed in the presence of CSL. Data for the 10% CSL (v/v) condition shown in Fig. 3b are depicted again in Fig. 4 for comparison.

Sugar utilization rates, MA titers, and MA productivities (Fig. 4b–e) increased with increasing levels of CSL in the media up to 5 g L^{-1}. At 96 h, the total sugar consumption was 78.9 g L^{-1}, 95.6 g L^{-1}, and 108.9 g L^{-1} for CSL levels of 0, 1 and 5% (v/v) CSL, respectively. However, the total sugar consumption was lower at 10% CSL compared to 5% CSL (v/v) (87.9 g L^{-1} and 102.9 g L^{-1} at 78 h, respectively, which is the time that the cultivation ended for the 10% CSL experiment). Furthermore, the cells in the 10% CSL condition exhibited a substantial decrease in cell density (Fig. 4a) and a deceleration in sugar utilization at 48 h compared to a higher sugar utilization rate at 5% (v/v) (Fig. 4b and c), suggesting a potential inhibitory effect of CSL at a concentration of 10%. MA titers increased from 30.1 g L^{-1} (0% CSL) to 47.2 g L^{-1} when supplementing media with 5% (v/v) CSL, which corresponds to over a 50% improvement. The different concentrations of CSL did not considerably impact the carbon molar yield of MA in this experimental setup (Fig. 4f). Overall, given the benefits observed at a CSL concentration of 5% over 10%, we selected the 5% as optimal for further work.

KH083 performance in sugar hydrolysate derived from corn-stover declines compared to mock hydrolysate

We next sought to demonstrate the production of MA from a lignocellulose-derived hydrolysate. The sugar hydrolysate was generated from corn stover using deacetylation, mechanical refining, and enzymatic hydrolysis (DMR-EH).[22] Typically, the glucose-to-xylose mass ratio in hydrolysates from the DMR-EH process is 2 : 1 (g/g),[22] which was the ratio used for the formulation of mock hydrolysate in the previous experiments.

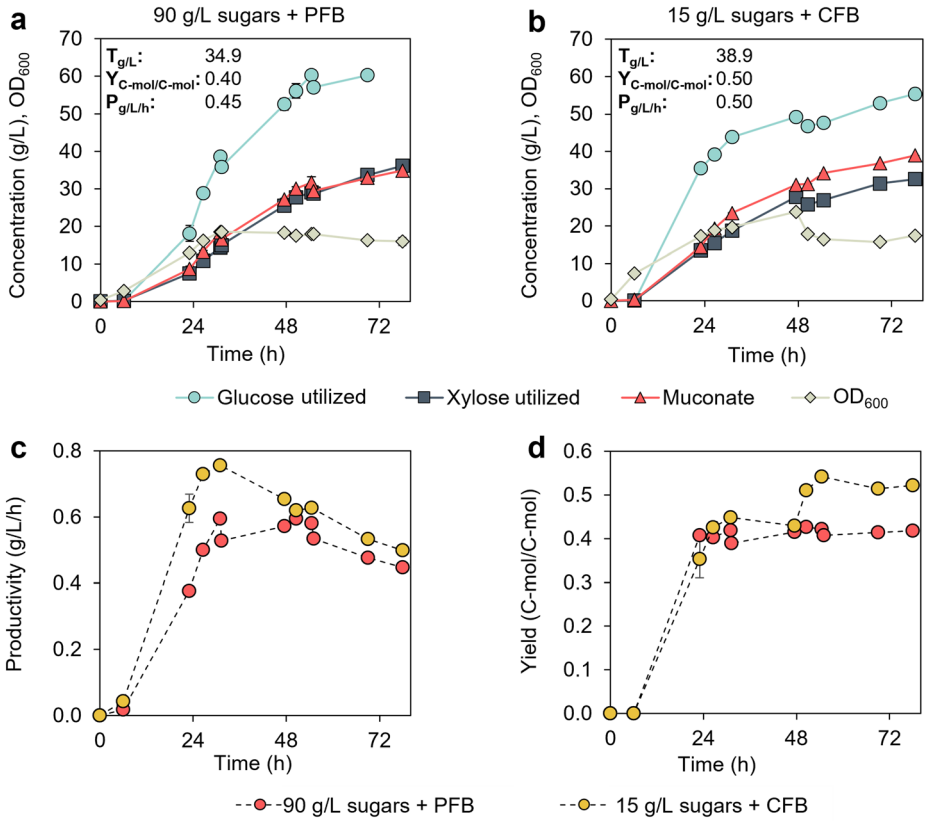

Fig. 3 Bioreactor profiles of KH083 from cultivations initiated and controlled at different sugar concentrations. Glucose and xylose utilization, bacterial growth (OD_{600}), and MA production in bioreactor cultivations conducted at (a) high initial sugar concentrations (90 g L^{-1}) and pulsed fed-batch mode (PFB) and (b) low initial sugar concentrations (15 g L^{-1}) and continuous fed-batch mode (CFB). Final MA titers (*T*), productivities (*P*), and yields (*Y*) corresponding to these cultivations at 78 h are provided in the graphs. Profiles for (c) MA productivities (g L^{-1} h^{-1}) and (d) MA yields (C-mol) are shown as a function of time from the two cultivation strategies. Modified M9 media supplemented with 10% (v/v) CSL was used in all cases. The glucose-to-xylose ratio was 2 : 1 (g/g). Glucose and xylose concentration profiles in the bioreactors are shown in Fig. S3.† The data points represent the average of biological duplicates, and the error bars represent the absolute error between duplicates. FB = fed-batch. All data in this figure are provided in ESI 1.†

However, the hydrolysate produced here contained a lower glucose-to-xylose ratio (1.5 : 1 g/g, Table S1†). Therefore, we conducted a parallel cultivation in mock hydrolysate to ascertain if sugar ratio impacts the bacterial performance. For this demonstration, we used a fed-batch mode controlled at low sugar concentrations in M9 media supplemented with 5% (v/v) CSL. KH083 performed similarly at glucose-to-xylose ratios of 1.5 : 1 (Fig. 5a) and 2 : 1 (Fig. 4), which implies that variations in sugar ratios at the tested range do not significantly affect bioprocess performance. In contrast, titers, yields, and productivities decreased in corn stover hydrolysate (Fig. 5b) compared to mock hydrolysate (Fig. 5a). Although OD_{600} values were similar between cultivations, both glucose and xylose utilization rates were slower in the hydrolysate, which resulted in lower final MA production rates (0.44 instead of 0.51 g L^{-1} h^{-1}) and titers (36.4 instead of 47.6 g L^{-1}) compared to the mock hydrolysate (Fig. 5). In addition, C-mol yields of MA also decreased. The reason for the observed decrease in performance remains unclear, as the hydrolysate used here lacks typical inhibitory sugar dehydration products present in acidic pretreatment processes.[22] The organic acids detected in this hydrolysate were lactic and acetic acid, albeit at concentrations significantly lower than those of the sugars (500 g L^{-1} sugars *versus* 9 g L^{-1} of lactic acid and 1 g L^{-1} of acetic acid, Table S1†). *P. putida* can utilize both lactic and acetic acid as carbon sources,[23,24] and acetate can be consumed simultaneously with sugars[23] suggesting that the presence of unknown components likely are the cause of these differences.

Scaling up MA production by KH083 from 0.5 L to 150 L bioreactors

We also tested the performance of KH083 at the 150 L scale. To maximize oxygen transfer in the bioreactor, we initiated the cultivation at a working volume of 90 L to ensure that both impellers were fully submerged. However, the maximum working volume in this bioreactor is 130 L, which did not allow us to keep the same volume ratio in the batch and fed-batch phase than that used at the bench scale (0.5 L) in optimal conditions. Therefore, to be able to achieve high MA titers, we started the batch phase at a high initial sugar con-

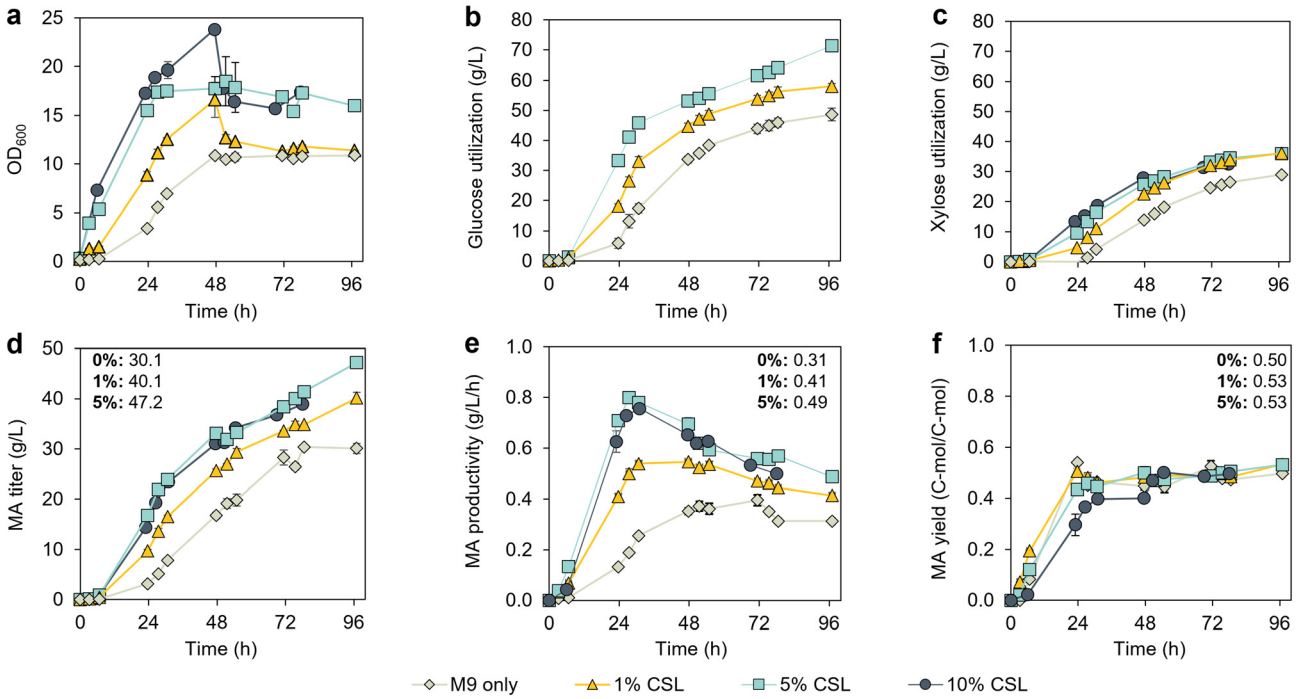

Fig. 4 Performance evaluation of KH083 in continuous fed-batch mode at different concentrations of corn steep liquor (CSL) in 0.5 L bioreactors. Bioreactor profiles show (a) bacterial growth (OD_{600}), (b) glucose utilization, (c) xylose utilization, (d) MA production, (e) MA productivity, and (f) MA yield for cultivations at different CSL concentrations. Profiles from 10% CSL (v/v), which correspond to the experiment conducted in Fig. 3 in continuous fed-batch mode, are also shown for comparison. Final titers, productivities, and yields correspond to 97 h for 0, 1, and 5% (v/v) CSL and are displayed in the corresponding panel. The glucose-to-xylose ratio was 2 : 1 (g/g). Glucose and xylose concentration profiles in the bioreactors are shown in Fig. S4.† The data points are the average of biological duplicates, and the error bars represent the absolute error between duplicates. All data in this figure are provided in ESI 1.†

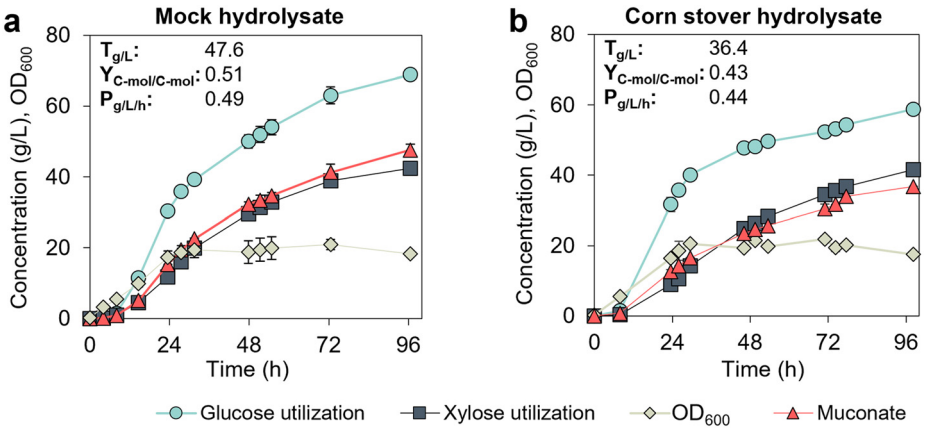

Fig. 5 Performance of KH083 on sugar hydrolysate derived from corn stover and mock hydrolysate. Bioreactor profiles for bacterial growth (OD_{600}), sugar utilization, and muconate production are shown for cultivations conducted in continuous fed-batch mode on (a) mock hydrolysate and (b) corn stover hydrolysate at glucose-to-xylose ratios of 1.5 : 1 (g L^{-1}). Final MA titers (*T*), productivities (*P*), and yields (*Y*) corresponding to mock and corn stover hydrolysate cultivations at 96.5 h and 98 h, respectively, are provided in the graphs. CSL concentration in batch and fed-batch media is 5% (v/v). Glucose and xylose concentration profiles in the bioreactors are shown in Fig. S5.† The data points represent the average of biological duplicates, and the error bars represent the absolute error between duplicates. All data in this figure are provided in ESI 1.†

centration (100 g L^{-1} mock hydrolysate plus 5% v/v CSL) and then, sugars and 5% v/v CSL were fed in a continuous mode (Fig. S6†). Considering these experimental differences, we also evaluated the same cultivation condition, and used the same seed train, at the bench scale (0.5 L bioreactors) to compare the effect of scaling on the performance metrics.

The performance of KH083 at the bench scale (Fig. 6a) was reduced compared to our optimum performance metrics

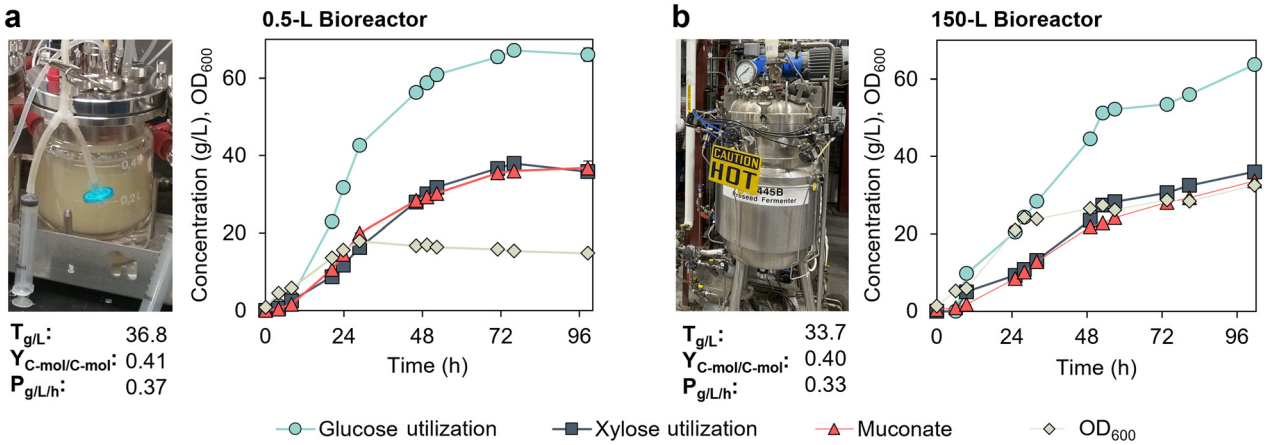

Fig. 6 Scaled-up MA production by *P. putida* KH083 from 0.5 L to the 150 L bioreactors. Bioreactor profiles for bacterial growth (OD_{600}), sugar utilization, and muconate production are shown for cultivations conducted in continuous fed-batch mode in a (a) 0.5 L bioreactor and (b) 150 L bioreactor. Final MA titers (*T*), productivities (*P*), and yields (*Y*) corresponding to 0.5 L and 150 L cultivations at 98.5 h and 101.5 h, respectively, are provided in the graphs. The glucose-to-xylose ratio was 2 : 1 (g/g). CSL in batch and fed-batch media was 5% (v/v). Glucose and xylose concentration profiles in the bioreactors are shown in Fig. S5.† Data for the 0.5 L bioreactor show the average of biological duplicates and error bars represent absolute error between duplicates. Data for the 150 L scale bioreactor correspond to a single cultivation. All data in this figure are provided in ESI 1.†

(Fig. 4), with 5% (v/v) CSL, most likely due to the high initial sugar concentrations (as previously observed in the pulsed fed-batch strategy, Fig. 3a). Regardless, we achieved similar metrics at 150 L to those observed at the 0.5 L scale (Fig. 6). Overall, at the 150 L scale, the final MA titer, productivity, and C-mol yield were 33.7 g L^{-1}, 0.33 g L^{-1} h^{-1}, and 0.40 C-mol C-mol^{-1}, respectively (Fig. 6b). Despite demonstration of consistent performance upon scale-up, it is noteworthy that the initial MA productivity was significantly higher at the 0.5 L scale, reaching 14.5 g L^{-1} of MA at 25 h compared to 8.5 g L^{-1} at 25 h at the 150 L scale. Interestingly, initial bacterial growth was higher at the 150 L scale, which could explain a decreased carbon flux to product. Dissolved oxygen was over 20% in both cases (Fig. S7†), so we do not attribute these differences to limitations in oxygen transfer at the larger scale.

Process modeling suggests that bio-based AA can approach cost parity with fossil-derived AA

Based on the promising experimental results obtained here, we further assessed the economic and environmental implications for MA production from lignocellulosic-derived sugars and its subsequent catalytic hydrogenation to AA. For that, a process model was developed in Aspen Plus V14 (AspenTech), in which mixed sugars are used as the primary carbon source for the process (Fig. 7a).

For sugar production, we modeled hydrolysates sourced from a facility that processes 2000 dry tons of corn stover per day with either two-stage DMR,[25,26] deacetylation and dilute acid (DDA),[27] or dilute acid (DA)[28] pretreatments. As shown in the simplified process flow diagram in Fig. 7a, the process starts with a seed train in bioreactors fed with mixed sugars from corn stover alongside sources of N and P required for growth, namely ammonia and diammonium phosphate. CSL is also added at concentrations following the experimental conditions, with the respective fermentation metrics (titer, productivity, and yield) being modified accordingly. Subsequently, an ultrafilter removes 99.5% of the solids, with a portion of the aqueous phase lost in the process, modeled at 10%. A low-pH crystallization recovers 96.2% of MA at 15 °C, which is redissolved in ethanol and then catalytically hydrogenated at 85 °C to yield AA with 100% yield.[29,30] The final AA product is separated with another crystallizer. The process model was used to inform the mass and energy balances required to determine the relevant metrics associated with the synthesis of MA and AA, including the minimum selling price (MSP) and greenhouse gas (GHG) emissions, and to estimate the influence of various process parameters on those metrics.

Compared to previous studies,[11,14] the effect of improving fermentation metrics through the addition of CSL up to 5% (v/v) ultimately contributed to a reduction in MSP for both MA and AA (Fig. 7b). While CSL is more expensive than ammonia (the main source of nitrogen in the modeled large-scale process) on a per mass of nitrogen basis, CSL boosts fermentation metrics beyond the threshold required to offset the slightly higher costs of this media component. When using DMR-based sugars, the baseline case for the assessment in this study, a MSP of $2.88 per kg of AA is achieved in M9 medium with 5% (v/v) CSL. Due to the potential of MA as a platform chemical for multiple applications besides AA,[2,31] the MSP of MA was calculated by altering the boundary for assessment (stopping prior to MA hydrogenation to AA) (Fig. 7b). As expected, the MSP of MA is consistently lower by 3–7% than that of AA, with an estimated MSP of $2.70 per kg with the addition of 5% (v/v) CSL to the bioreactors. Cost parity with the upper range of fossil-based AA prices while using DMR sugars as the feedstock could be potentially achieved with an estimated rate of 1 g L^{-1} h^{-1} (while maintaining the same yield as that obtained in the base case) or with a yield of

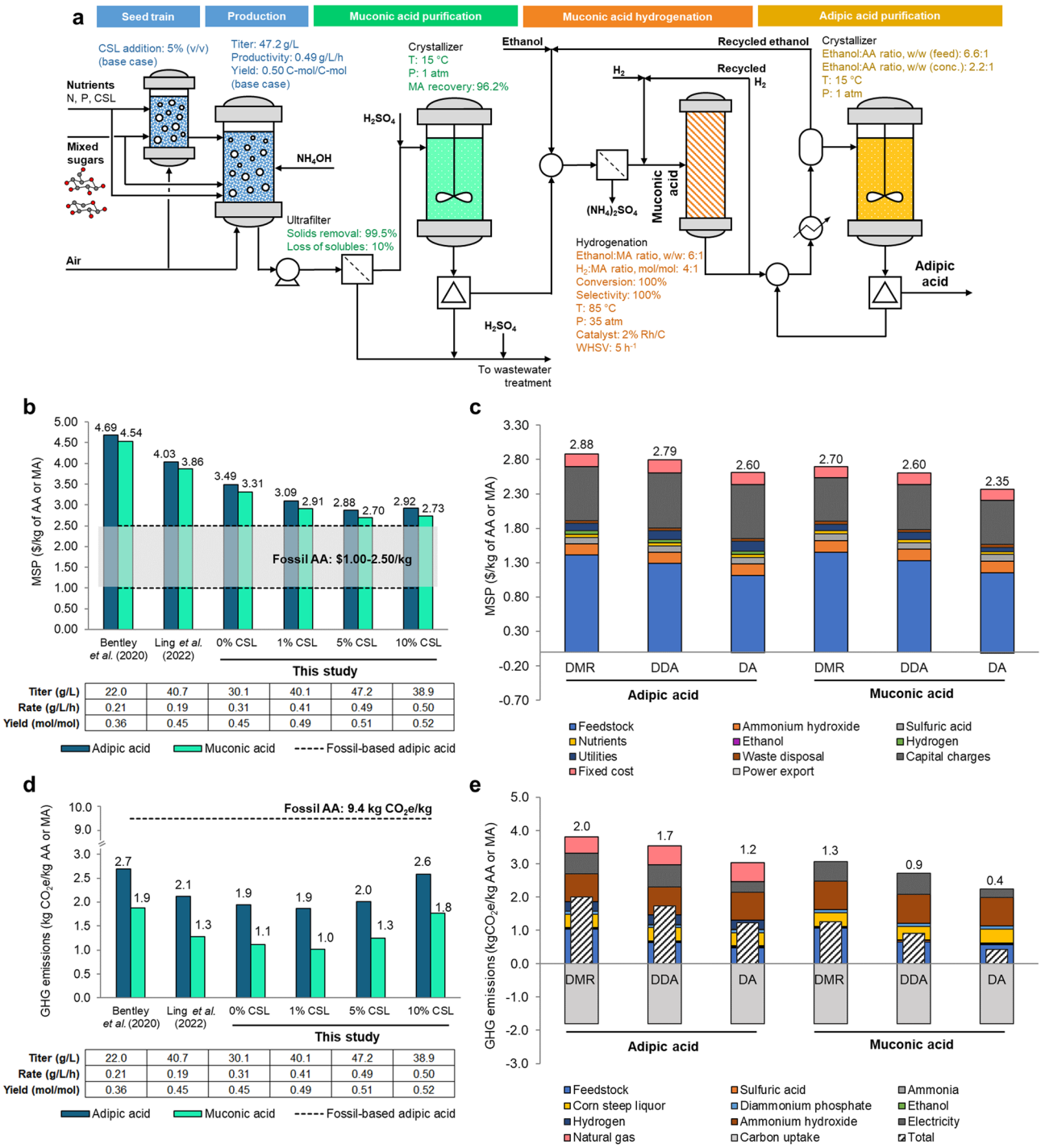

Fig. 7 Process model, economics, and GHG emissions for MA and AA production from lignocellulosic sugars. (a) Framework for the process simulation of MA and AA production from mixed sugars. Parameters used in process simulations are detailed for the main equipment. (b) Comparison between minimum selling prices (MSPs) of AA (blue) and MA (teal) produced from DMR sugars using bioprocess metrics from previous publications (Bentley *et al.*[11] and Ling *et al.*[14]) and those determined in this study with different CSL addition ratios. (c) Contributions to the MSP of AA as synthesized using the optimal cultivation conditions verified in this study: addition of 5% (v/v) CSL to modified M9 media and residence time of 96 h for three corn stover pretreatment methods: DMR, DDA, and DA. (d) Comparison of GHG emissions for AA (blue) and MA (teal) production from DMR sugars using bioprocess metrics from previous publications (Bentley *et al.*[11] and Ling *et al.*[14]) and those determined in this study with different CSL addition ratios and cultivation times. (e) Breakdown of the GHG emissions for MA and AA produced from DMR, DDA, and DA sugars for the best-case scenario of 5% (v/v) CSL. All data in this figure are provided in full in ESI 1.†

0.68 mol mol^{-1} (while keeping the rate at the base value of 0.49 g L^{-1} h^{-1}). We also modeled two different pretreatment options that yield mixed sugars at lower costs (DDA and DA). Sugars from DDA-based biorefineries could further reduce the MSPs of AA and MA by ~3% to $2.79 per kg and $2.60 per kg, respectively; switching to mixed sugars from DA could further lower MSPs of AA and MA by ~12%, resulting in estimated MSPs of $2.60 per kg and $2.35 per kg, respectively (Fig. 7c). It is noteworthy that, historically, AA prices fluctuated significantly, ranging from $1.00 per kg in the early 2010s to $2.50 per kg as of 2024.[32,33] We also note that the fermentation metrics used in this study were derived using DMR hydrolysates and that employing hydrolysates from alternative pretreatment methods (*i.e.*, DDA and DA) in the production of AA and MA may result in lower performance metrics (as these methods are known to generate fermentation inhibitors[22]), which could impact the estimated MSPs.

Using this process model, the impact of bioconversion, separations, and upgrading operations were also evaluated (Fig. 7c). From a capital expenditures (CAPEX) standpoint, aerobic cultivation in the base case requires 52 bubble column bioreactors with capacity of 1000 m^3, which are priced at around $1.6 million each (uninstalled costs).[34] In terms of operational expenses (OPEX), the sugar cost is the main driver in the cost of AA, with ammonium hydroxide and sulfuric acid for neutralization, hydrogen for the hydrogenation of MA, cultivation nutrients, and utilities being lesser contributors to overall economics. The primary inputs and outputs of the baseline biorefinery design are shown in Table S7,† while a breakdown of the CAPEX is presented in Table S8.†[32,33]

LCA predicts that AA production from mixed lignocellulosic sugars can achieve substantial GHG emissions reductions

The R&D GHG emission results (Fig. 7d) were calculated using both The Greenhouse gases, Regulated Emissions, and Energy use in Technologies[35] (GREET®) model version 2023 (for which results are shown in the main text) and SimaPro/ecoinvent (results presented in the ESI†). Boundaries for assessment are shown in Fig. S8.† Similar to the MSP results, GHG emissions of MA are consistently lower by 31–46% than those of bio-based AA. This trend is expected as the processing of sugars to AA requires a higher consumption of energy (*i.e.*, natural gas) and chemicals (*e.g.*, ethanol and especially hydrogen) relative to a biorefinery producing MA. The estimated GHG emissions for both AA and MA in this study improved over the previous works by Bentley *et al.*[11] and Ling *et al.*[14] (Fig. 7d) up to the addition of 1% and 5% (v/v) CSL to the cultivation media, with the last case (10% v/v CSL) predicted to exhibit higher GHG emissions compared to using the metrics from Ling *et al.*[14] Details of the GHG emission contributions for AA and MA and for selected sensitivity analyses can be found in the ESI (Tables S9–S11 and Fig. S9–S14† for AA and MA). While an increase in CSL consumption boosts cultivation metrics, it brings a non-negligible contribution towards the GHG emissions of either MA or AA production for CSL addition levels above 1% v/v, despite minimizing the consumption of both ammonia and diammonium phosphate as nutrient sources. This trade-off drives the differences among all cases, especially in the cases with higher CSL supplementation.

Comparing the results for bio-derived AA with its fossil-based counterpart, the GHG emissions can be reduced by 71%, 77%, 79%, 80%, 79%, and 72% for each of the cases shown in Fig. 7d, respectively. Fig. 7e compares the GHG emissions for both AA and MA with 5% (v/v) CSL addition based on converting sugars from the three different pretreatment methods analyzed so far. DA pretreatment presents some benefits as feedstock's impact is lower than both DMR or DDA pretreatment strategies. The GHG emissions of AA decrease by 25% and 37% compared to DDA and DMR pretreatments, respectively, while this switch could represent reductions of 51% and 65% for MA. In addition to GHG emissions, fossil energy consumption and water consumption were included in this analysis and the results are presented in the ESI (Fig. S15†).

Single-point sensitivity analyses highlight the main economic and GHG emissions drivers for bioprocess cost reduction

We then conducted a single-point sensitivity analysis for MSP (Fig. 8a), identifying MA yield from mixed sugars as the main factor affecting process economics. Improvement in productivity is also a significant economic driver, with titer being less impactful. Achieving a product yield of 0.6 mol mol^{-1} would translate to a reduction of more than $0.33 per kg in the MSP of AA, while a reduction to half of the yield achieved in the base case would incur an increase in MSP of $1.80 per kg. A variation of rate among the extremes of 0.2–2 g L^{-1} h^{-1} would impact the MSP of AA by +$0.66 per kg and −$0.33 per kg, respectively. As seen in Fig. 7c, increasing the MA productivity could lower the CAPEX of the bubble columns used in the cultivations: while there are diminishing economic returns after a threshold rate of 0.5 g L^{-1} h^{-1}, any improvements of the rate will further reduce MSP, although not linearly. Finally, attaining titers of up to 100 g L^{-1} of MA would reduce MSP by $0.10 per kg. Similarly, GHG emissions are driven mainly by the variation of yield (Fig. 8b), with values ranging from 1.73 $kgCO_2e$ per kg AA (*i.e.*, high yield case) to 3.94 (*e.g.*, low yield), which represents an 13% decrease and a 96% increase from the base case of 2.01 $kgCO_2e$ per kg of AA. Titer and productivity show minor effects on the GHG emissions of AA.

Another aspect of the process that could be considered for its large-scale deployment is the recovery of ammonium sulfate formed through the neutralization of ammonium hydroxide and sulfuric acid. While the baseline analyzed here does not carry out this operation, being able to reclaim this salt from the process wastewater would have an economic impact that is equivalent to that of advancing the fermentation rate to 2 g L^{-1} h^{-1}, meaning a reduction in MSP of AA of $0.33 per kg, independently of the source of mixed sugars. Accordingly, sulfate recovery could reduce the GHG emissions of AA to 1.56 $kgCO_2e$ per kg (22% less than the base case)

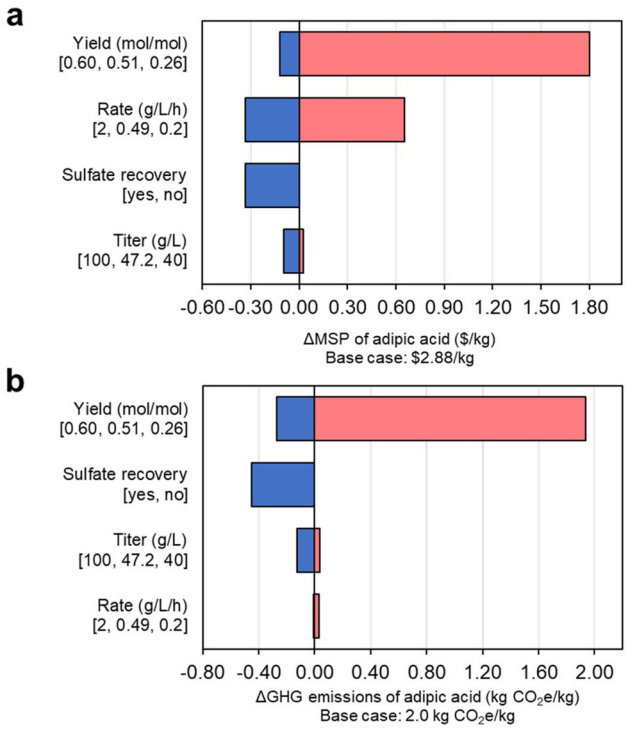

Fig. 8 Single-point sensitivity analysis of parameters related to MA fermentation over the (a) MSP and (b) GHG emissions of producing AA from DMR sugars. Baseline fermentation parameters to generate the MSP of $2.88 per kg of AA and the GHG emissions of 2.0 kg CO_2e per kg AA are presented in parentheses, while extreme range points are indicated below each label. All data shown in this figure are provided in full in ESI 1.†

because the total biorefinery emissions will be distributed between AA and ammonium sulfate based on their market-value share. The *E*-factor[36] for the baseline process is 2.42, with ammonium sulfate representing over half of the waste generated in the process (as detailed in the ESI 2†).

Discussion

The primary economic factors in the production of MA from lignocellulosic sugars – and identified as key drivers to make this process viable – are feedstock cost, capital charges, and the generation of waste salts. Capital charges include major contributions to MA yields and productivity, and our study demonstrates productivity enhancements that reduce AA MSP by $1.15 per kg compared to previous work.[14] CSL has been shown in various studies to enhance biocatalyst performance,[37–40] most likely due to the high concentration of amino acids. Similarly, its use in this study was critical for the overall improvements, with the addition of CSL corresponding to an MSP reduction of $0.61 per kg compared to the case where no CSL is added in the hydrolysate. This work also revealed that the use of sugars from DDA or DA pretreatment instead of DMR may further reduce MSPs of MA and AA if microbial performance metrics are similar among hydrolysates, bringing the costs relatively close to the current market prices of fossil-derived AA (which ranged between $1.10 per kg to $1.80 per kg in the United States between 2010 and 2020, with a more recent increase to $2.50 per kg in 2024).[32] We note that the performance metrics of KH083 in DMR hydrolysate were lower than those obtained in mock hydrolysate (the latter used as base case metrics for TEA). Therefore, understanding the origin of those differences and directing strain engineering efforts towards mitigating any inhibition from hydrolysates is warranted.

From an environmental standpoint, significant GHG emissions reductions were achieved for all cases investigated in this study, except when using 10% (v/v) CSL, compared to previous studies.[11,14] GHG emission savings of 0.26 and 0.35 kgCO_2e per kg for AA and MA, respectively, were achieved with DDA pretreatment compared to DMR pretreatment. Further reductions of 0.71 KgCO_2e per kg for AA and 0.81 kgCO_2e per kg for MA were attained with DA pretreatment. Fossil-based AA (9.4 kgCO_2e per kg) has high GHG emissions due to its use of petrochemical feedstocks derived from benzene and high N_2O emissions.[41] Overall, our LCA results indicate that significant emissions reductions (at least 71%) can be achieved by producing biobased AA, regardless of the bioreactor cultivation or pretreatment strategies, compared to fossil-derived AA. Lastly, this study shows that the comparison of GHG emissions breakdown between GREET and SimaPro for MA and AA (Fig. S12 and S13†) were similar between the two LCA tools, with variations due to differences in how these models account for the production and usage of sulfuric acid, hydrogen, and ammonium hydroxide.

P. putida has been shown to be an excellent biocatalyst capable of simultaneously metabolizing a wide range of substrates, including sugars, organic acids, and aromatic compounds.[17,20,42–46] In addition, here we demonstrate that the proportion of sugars, at either glucose-to-xylose ratios of 2 : 1 or 1.5 : 1, does not impact MA metrics in KH083. This is a key feature considering that sugar ratios vary in hydrolysates generated from different feedstock batches,[47] and that sugar ratios have been reported to negatively affect the performance of other bacteria.[48–50] Lastly, *P. putida* had been previously scaled to 72 L for MA production from mixtures of aromatic compounds derived from lignin, and showed a ten-fold decrease in MA productivity compared to bench scale.[51] Here, we demonstrate comparable final performance metrics of *P. putida* KH083 between 0.5 and 150 L bioreactors, despite lower initial MA productivities at the larger scale. Microenvironments can be generated within large-scale cultivations (*e.g.*, with variable oxygen, pH, and sugar levels), potentially impacting performance metrics. In fact, glucose and oxygen levels have been demonstrated to impact the growth of wild-type *P. putida* in scale-down systems that mimic microenvironments from large scale bioreactors.[52,53]

This study is subject to several limitations. Nutrient-rich media, such as CSL, may exhibit variations among batches, potentially impacting bioprocess metrics. We also acknowledge that CSL enhances the risk of microbial contamination

through spores present in the CSL. This was a noticeable issue in our first attempt to scale up MA production to 150 L as well as in the parallel 0.5 L cultivations. Therefore, we conducted nano-filtration (70 nm filter pore size) in addition to heat sterilization of CSL in our second attempt (Fig. 6) to eliminate spores. Related to scale-up, another limitation is the design of the bioreactor employed in this study, which did not allow us to replicate the optimal conditions identified at the 0.5 L scale for maximizing MA titers, rates, and yields. Thus, optimizing bioreactor design to enable lower volumes while maintaining appropriate oxygen transfer could lead to significant performance enhancements.

Based on the sensitivity analyses conducted in this study to reduce the MSP of AA and MA, future work will focus on further improving MA productivities and yields through strain and bioreactor engineering strategies. Additionally, capturing the waste salt or eliminating it through process engineering innovations will be also critical to the overall process. Together, this study highlights the potential of engineered *P. putida* to achieve high MA titers, productivities, and yields from mixed sugars and at the pilot scale in the presence of CSL, underscoring bioprocessing as a compelling approach to produce biochemicals from renewable sources.

Methods

Strain construction

A glycerol scrape of strain LC224[14] was inoculated into 4 mL LB (Miller) medium in a 15 mL culture tube and incubated overnight at 30 °C, 225 rpm. Cells were made electrocompetent by following the sucrose washing method as described by Choi *et al.*[54] Each transformation contained 50 μL of competent cells with around 500 ng of a plasmid previously constructed for deletion of *gacS* (pAW052)[55] or *gntZ* (pJH0002)[11] and was carried out in a Gene Pulser Xcell (Bio Rad) using 0.1 cm cuvette, 1.6 kV, 25 μF and 200 ohms as the settings. Immediately after electroporation, cells were resuspended in 950 μL SOC medium (New England Biolabs) and incubated 1–2 hours in a 1.5 mL microfuge tube at 30 °C and shaking at 225 rpm. The recovered cells were then centrifuged for 1 minute at 8000 rpm before removing 850 μL of the supernatant and plating the concentrated, resuspended cells onto LB agar (Lennox) plates with 50 μg mL^{-1} kanamycin. The downstream protocol of gene deletions was described in detail previously.[42] The kanamycin resistant gene *nptII* in plasmid backbones pk18sB[56] and pk18mobsacB[57] was used as the selection marker for the first round homologous recombination of plasmid into the chromosome. The *sacB* gene encoding the secreted enzyme levansucrase which confers sucrose sensitivity,[58] was used as the counterselection marker for the second homologous recombination of plasmid backbone out of the chromosome. Correct deletions were identified first through colony PCR using Q5 High Fidelity DNA polymerase (New England Biolabs). These PCR regions were then verified by Sanger sequencing (Genewiz).

Strain evaluation in plate reader and shaken flasks

We performed plate reader and shaken flasks experiments to investigate the performance of strains LC224, KH083, and KH099, in M9 medium (6.78 g L^{-1} Na_2HPO_4, 3 g L^{-1} KH_2PO_4, 0.5 g L^{-1} NaCl, 1 g L^{-1} NH_4Cl, 2 mM $MgSO_4$, 100 μM $CaCl_2$, 18 μM $FeSO_4$) supplemented with glucose (5.4 g L^{-1}) and xylose (2.3 g L^{-1}). For both experiments, seed cultures were initiated by inoculating cells from the surface of frozen glycerol stocks into 14 mL Falcon® tubes containing 5 mL of LB Miller medium. The inoculated cultures were incubated overnight at 30 °C and 225 rpm.[11] These cultures were then inoculated into 125 mL baffled shaken flasks containing 10 mL LB Miller medium to an initial OD_{600} of 0.2, to generate a second seed culture, which was then incubated at 30 °C and 225 rpm for 4–6 hours to reach an OD_{600} of approximately 4. The second seed cultures were centrifuged down in 15 mL centrifuge tubes at 4000*g* for five minutes and washed twice using M9 medium. The washed cells were then concentrated to 1 mL using M9 medium before inoculation into plates or shaken flasks. For the plate reader experiment, the concentrated cell cultures were adjusted to an OD_{600} of 3.0, and then 10 μL OD_{600}-adjusted cell cultures were inoculated into each well containing 290 μL M9 medium supplemented with 30 mM glucose and 15 mM xylose, to reach an initial OD_{600} of 0.1. For shaken flasks experiment, the concentrated cell culture was inoculated into a 125 mL baffled flask containing 25 mL of modified M9 minimal medium supplemented with 30 mM glucose and 15 mM xylose, to an initial OD_{600} of 0.1. At each sampling time point the pH of each flask was measured using a Horiba Compact Laquatwin pH-33 Compact pH meter and adjusted to between 7.0–7.2 using 1 N NaOH.

Seed preparation for cultivations conducted in 250 mL shaken flasks and 0.5 L bioreactors

Strains were revived from glycerol stocks by scrapping the surface of the vials and inoculating in 250 mL baffled flasks containing 50 mL LB (Miller) medium. The seed cultures were incubated overnight at 30 °C and 225 rpm for approximately 16 h. We then harvested the cells to inoculate bioreactors at an initial OD_{600} 0.2 by washing and concentrating cells from the overnight culture in 5 mL of modified minimal media (M9). Unless otherwise stated, modified M9 media consisted of 13.56 g L^{-1} Na_2HPO_4, 6 g L^{-1} KH_2PO_4, 1 g L^{-1} NaCl, 2 g L^{-1} $(NH_4)_2SO_4$, 2 mM $MgSO_4$, 100 μM $CaCl_2$ and 36 μM $FeSO_4$.

Evaluation of the effect of sugar and CSL concentration on KH083 in shaken flasks

P. putida KH083 was evaluated in shaken flasks experiments with different media compositions. Cells were inoculated at an initial OD_{600} of 0.2 in 250 mL shaken flasks containing 50 mL of modified M9 media supplemented with an initial sugar concentration of 15, 75, 100, or 125 g L^{-1} (glucose-to-xylose ratio of 2 : 1, g/g) with and without 10% (v/v) CSL. CSL (SOLULYS 095K, Roquette™) was prepared at a concentration of 200 g L^{-1} and then autoclaved at 121 °C for 1 h. After cooling, the

solids were separated by centrifugation (13 880*g* for 30 minutes) and the supernatant was further autoclaved at 121 °C for 1 h. Cultivations were controlled at 30 °C and shaking was kept at 225 rpm. All shaken flasks cultivations were performed in duplicate.

General characteristics for cultivations conducted in 0.5 L bioreactors

Bench scale cultivations in bioreactors were conducted in 0.5 L vessels in a BioStat-Q Plus system (Sartorius Stedim Biotech). Three drops of sterile Antifoam 204 (Sigma Aldrich, United states) were added to the batch media prior to inoculation. Cultivations were controlled at 30 °C, at pH 7 with 4 N NH_4OH (unless otherwise specified) and were initially sparged with air at 300 mL min^{-1}. Initial dissolved oxygen (DO) saturation level initiated at 100%, at a minimum agitation of 350 rpm. Once DO dropped to 30%, DO was automatically controlled at 30% by automatic changes in the agitation speed. Samples were collected following a sterile technique to measure bacterial growth (OD_{600}) and concentration of metabolites. In general, cultivations ended when the utilization of sugars was negligible, as confirmed by an offline sugar analyzer (YSI 2900 Series). Specific details for each experimental campaign in bioreactors are detailed below.

Bioreactor cultivations in batch mode for strain evaluation

Initial strain evaluation between LC224 and KH083 in bioreactors was conducted in batch mode. The batch media volume was 250 mL and contained modified M9 minimal media, supplemented with 75 g L^{-1} of sugars (50 g L^{-1} glucose, 25 g L^{-1} xylose and 2.2 g L^{-1} arabinose). The batch cultivation was terminated once all the sugars were consumed, which was signaled by a sudden increase in the DO level.

Bioreactor cultivations in fed-batch mode controlled at high sugar concentrations

The batch media (250 mL) contained modified M9 media supplemented with 90 g L^{-1} of sugars (57.8 g L^{-1} glucose, 29.5 g L^{-1} xylose and 2.7 g L^{-1} arabinose), and 10% CSL (v/v). Once the total sugar in the bioreactor dropped between 15 and 25 g L^{-1}, the fed-batch phase initiated. The media was spiked with a concentrated sugar solution to raise the sugar level to 50–60 g L^{-1} (Fig. S3†). The feeding media contained 300 g L^{-1} glucose, 153 g L^{-1} xylose, 14 g L^{-1} arabinose, and 10% CSL (v/v). The feeding media was adjusted to pH 7 with NaOH. Antifoam 204 was added to feeding media at concentration of 4 mL L^{-1}.

Bioreactor cultivations in fed-batch mode controlled at low sugar concentrations

The batch media (250 mL) consisted of modified M9 media and 15 g L^{-1} of sugars (9.6 g L^{-1} glucose, 4.9 g L^{-1} xylose and 0.5 g L^{-1} arabinose), supplemented with varying levels of CSL (0, 1%, 5% and 10% v/v). The feeding media contained 467 g L^{-1} of sugars (300 g L^{-1} glucose, 153 g L^{-1} xylose and 14 g L^{-1} arabinose), also supplemented with the same level of CSL as that utilized in the batch media. Antifoam 204 was added to feeding media at concentration of 4 mL L^{-1}. The feeding initiated at 7 h after inoculation, to maintain a total sugar concentration between 5 g L^{-1} and 20 g L^{-1} (Fig. S4†). The feeding was continuous, but the rate was adjusted manually according to the sugar consumption rate, estimated from the reading of an offline sugar analyzer (YSI 7100 MBS).

Bioreactor cultivation in batch mode with 5% CSL (v/v) as the sole carbon source

The batch media (250 mL) contained modified M9 media supplemented with 5% CSL (v/v) as the sole carbon source. Although the starting pH was 7, there was an increase in the pH of the broth up to 7.4 as CSL was utilized. The cultivation was terminated at 6.7 hours.

Bioreactor cultivations in fed-batch mode with corn stover hydrolysate and mock hydrolysate

We used corn stover sugar hydrolysate prepared in a similar manner to that reported by Salvachúa *et al.*[21] and Chen *et al.*[22] The initial batch media (250 mL) consisted of modified M9 supplemented with 15 g L^{-1} of hydrolysate or pure sugars (9.2 g L^{-1} glucose and 5.8 g L^{-1} xylose and 0.4 g L^{-1} arabinose) and 5% CSL (v/v). The feeding media consisted of 285 g L^{-1} glucose, 175 g L^{-1} xylose and 14.7 g L^{-1} arabinose as well as 5% (v/v) CSL and was adjusted to pH 7 with 4 N NaOH. Antifoam 204 was added to feeding media at concentration of 4 mL L^{-1}. The feeding initiated at 7 h after inoculation, to maintain a total sugar concentration between 15 g L^{-1} and 25 g L^{-1} (Fig. S5†). The feeding was continuous, but the rate was adjusted manually according to the sugar consumption rate, estimated from the reading of an offline sugar analyzer (YSI 7100 MBS).

Bioreactor cultivations in fed-batch mode at the pilot scale in a 150 L bioreactor and at the 0.5 L scale

The seed train for both the 150 L and 0.5 L scale bioreactors consisted of: (seed 1) scrape of glycerol stock to 250 mL flasks with 50 mL LB (Miller) and incubated overnight at 30 °C and 225 rpm for 16 h, (seed 2) 0.5 L bioreactor with 250 mL of LB (Miller) inoculated at an OD_{600} of 0.2 from seed 1 and incubated for 3.5 hours at 30 °C and at pH 7 (controlled with 4 N NH_4OH) and DO controlled at 30% by agitation, and (seed 3) 10 L bioreactor (Eppendorf) with 9 L of modified M9 and 50 g L^{-1} total sugars (glucose-to-xylose ratio of 1 : 2, g/g), inoculated at an OD_{600} of 0.2 from seed 2, incubated at 30 °C and pH 7 (controlled with 4 N NH_4OH) and DO controlled at 30% by agitation. Seed 3 ended when OD_{600} was 10, at ~16 h. Then, we inoculated both the 0.5 L and 150 L vessels at an initial OD_{600} of 1 by 10% (v/v) direct transfer of broth from seed 3.

The pilot scale cultivation was performed in a 150 L vessel with an initial batch volume of 90 L. The batch media consisted of modified M9 media supplemented with 91.7 g L^{-1} of sugars (58.7 g L^{-1} glucose, 30.8 g L^{-1} xylose and 2.2 g L^{-1} arabinose) and 5% CSL (v/v). The feeding media consisted of 423 g L^{-1} of sugars (272.4 g L^{-1} glucose, 137.9 g L^{-1} xylose,

and 12.7 g L^{-1} arabinose) supplemented with 5% CSL (v/v). To avoid contamination at 150 L scale due to presence of spores in CSL, CSL was subjected to nanofiltration at a pore size of 70 nm using a ceramic membrane (α-Al_2O_3, Rauschert, USA). The cultivation was controlled at 30 °C, at pH 7 (with 7 N NH_4OH), and was sparged with air at 90 L min^{-1}. The DO saturation levels were controlled automatically at 30% by agitation. The feeding initiated at 49 hours and the rate was adjusted to control sugars between 15 and 30 g L^{-1} (Fig. S6†). The feeding was continuous, but the rate was adjusted manually according to the sugar consumption rate, estimated from the reading of an offline sugar analyzer (YSI 2900 Series). We collected samples following a sterile technique to measure bacterial growth and metabolite concentrations. The same media composition (including the water source) and bioreactor control parameters were used for the batch phase (250 mL) and feeding media in the 0.5 L bioreactors.

Calculation of bioreactor parameters

MA titers are reported as the total MA production (*cis*,*cis* and *cis*, *trans* muconic acid) analyzed at the end of the cultivation. Productivities are calculated as the coefficient of the final MA titer divided by the time at the end of the cultivation. MA C-mol yields were calculated as the coefficient of C-mols from MA and the C-mols from utilized from glucose, xylose, and CSL, assuming full utilization of TOC in CSL. Mol yields were calculated as MA mols divided by mols of glucose and xylose utilized. Yields accounted for dilution due to feeding and base addition for pH control.

Metabolite analysis

cis,*cis* and *cis*,*trans* MA isomers were analyzed using methods detailed previously.[14,59] MA concentrations reported in this study represent the total concentration of both isomers. Glucose and xylose were quantified simultaneously by HPLC with refractive index detection coupled with an Aminex HPX-87H column (Bio-Rad) as reported before.[14,60]

Compositional analyses for hydrolysate

The composition of the corn stover derived hydrolysate (Table S1†) was analyzed following a procedure in the NREL standard laboratory Analysis Procedure (LAP No. NREL/TP-510-42623).[61]

Techno-economic analysis

Process simulations were carried out using the Aspen Plus V10 software (AspenTech). Dedicated biorefineries were simulated to represent the conversion of 2000 dry tons of corn stover per day into mixed sugars through pretreatment and enzymatic hydrolysis steps, followed by their aerobic fermentation to MA and further upgrading to AA. General modeling assumptions for biomass handling, pretreatment, on-site enzyme production, enzymatic hydrolysis, and cogeneration of heat and power (CHP) were set consistent with NREL's 2018 biochemical design report. Parameters related to the bioconversion of sugars to MA and upgrading to AA were modeled after Johnson 2019.[20] Further details are presented in the ESI (Tables S5 and S6†).

Material and energy balances obtained from process simulation efforts were then used as inputs to determine capital expenditures (CAPEX) and operational expenses (OPEX) associated with the integrated biorefining process. Finally, discounted cash flows (DCFs) were established to assess the economic performance of the biorefineries in question, aiming at estimating the minimum selling price (MSP) of MA and AA, which corresponds to the sales price required to balance the economics of the facility (*i.e.*, net present value of zero) over a 30-year lifetime. Additional details concerning process simulation and TEA results are shown in Tables S5–S8, and in the ESI 2.†

Life cycle assessment

The material and energy balances for the biorefinery model were obtained from the Aspen process simulations and fed into the R&D GREET LCA tool,[35] and the feedstock production, processing, and logistics were leveraged from the R&D GREET feedstock data sets (Argonne, 2023). As a LCA tool comparison and sensitivity study, we also conducted an LCA using SimaPro software to assess the life cycle impacts based on the same life cycle inventory (LCI) (Fig. S9–S11†). SimaPro includes the ecoinvent v3 database[62] and the DATASMART LCI package, which contains background processes relevant to our study. The functional unit for this study was chosen as one kg of bioproduct output and the GHG emission results were presented in terms of kilograms (kg) of CO_2-equivalent per kg of adipic or muconic acid produced ($kgCO_2e$ per kg). The results were compared to the petroleum-based AA calculated from the GREET model on a cradle-to-gate basis. The emissions of carbon dioxide (CO_2), methane (CH_4), and nitrous oxide (N_2O) are included in the scope with global warming potential calculated on a basis of the IPCC Fifth Assessment Report values for the 100-year time horizon, 1, 30, and 273 g CO_2e per g, respectively[63] (IPCC, 2022). For this analysis, we used the market-based co-product method to allocate the emissions and energy burdens between the economic values of the main product and co-products (*e.g.*, electricity for the mixed sugar intermediate part). Additional details regarding the LCA, as well as a comparison between the GREET model and SimaPro GHG emission results, are presented in the ESI (Tables S9–S11 and Fig. S8–S14†).

To estimate LCA results, we modeled the GHG emissions incurred in the conversion of corn stover to the mixed sugar intermediate first, and then incorporated this burden in the modeling of the bioconversion and upgrading operations to the bioproducts (Fig. 7a). Therefore, in Fig. 7e, the environmental burden associated with the feedstock corresponds to the mixed sugar intermediate as opposed to corn stover (the reader is referred to the 'Life cycle assessment' section in the ESI† for the full account on determining the GHG emissions of DMR, DDA, and DA mixed sugar intermediates using different LCA tools and product handling methods, namely Table S11 and Fig. S11, S14†).

Author contributions

G. T. B. and D. S. conceived the project. S. C. M., B. C. K., P. T. B., E. C. D. T., G. T. B., and D. S. designed the study. S. C. M. and C. M. K. conducted cultivations in flasks and bench scale bioreactors. B. C. K., P. T. B., E. C. D. T. conducted TEA and LCA analyses. C. L., K. V. H., and C. W. J. designed and constructed plasmids, and/or genetically engineered *P. putida*. K. J. R. and M. A. I. conducted muconate and sugar analyses *via* HPLC-based analytics. S. C. M., C. M. K., C. A. S., R. L., V. S. N., and D. S. designed and/or conducted the pilot scale cultivation in the 150 L bioreactor. S. C. M., B. C. K., P. T. B., and D. S. wrote the manuscript which has been edited and approved by all authors.

Data availability

All key data is provided in the manuscript or the ESI.† Any additional information can be requested from the corresponding author.

Conflicts of interest

There are no conflicts to declare.

Acknowledgements

This work was authored in part by Alliance for Sustainable Energy, LLC, the manager and operator of the National Renewable Energy Laboratory for the U.S. Department of Energy (DOE) under Contract No. DE-AC36-08GO28308. This work was also partially authored by Argonne National Laboratory, which is managed by UChicago Argonne, for the U.S. DOE under contract DE-AC02-06CH11357. Funding was provided by the U.S. Department of Energy Office of Energy Efficiency and Renewable Energy Bioenergy Technologies Office (BETO) for the Agile BioFoundry (ABF). The authors gratefully acknowledge the support and direction of Gayle Bentley at BETO. We thank Kyleigh Newman-Rosenthal and Patrick Saboe for conducting the nanofiltration of CSL. We thank Dan Schell, Mike Baker, and the pilot plant team at NREL for fruitful conversations and advice prior to the scale-up. We thank Sean P. Woodworth, Hannah Alt, and Alex Benson for their support with metabolite analyses. We thank Ryan Davis for his discussions regarding the TEA. We thank Allison Z. Werner for sharing the plasmid pAW052 for this study. We thank Roquette for sharing CSL samples (SOLULYS 095K, Roquette™) for this study.

References

1 K. M. Draths and J. W. Frost, Environmentally compatible synthesis of adipic acid from D-glucose, *J. Am. Chem. Soc.*, 1994, **116**(1), 399–400.

2 I. Khalil, G. Quintens, T. Junkers and M. Dusselier, Muconic acid isomers as platform chemicals and monomers in the biobased economy, *Green Chem.*, 2020, **22**, 1517–1541.

3 R. Lu, F. Lu, J. Chen, W. Yu, Q. Huang, J. Zhang, *et al.*, Production of diethyl terephthalate from biomass-derived muconic acid, *Angew. Chem., Int. Ed.*, 2016, **55**(1), 249–253.

4 D. R. Vardon, M. A. Franden, C. W. Johnson, E. M. Karp, M. T. Guarnieri, J. G. Linger, *et al.*, Adipic acid production from lignin, *Energy Environ. Sci.*, 2015, **8**(2), 617–628.

5 N. Z. Xie, H. Liang, R. B. Huang and P. Xu, Biotechnological production of muconic acid: current status and future prospects, *Biotechnol. Adv.*, 2014, **32**(3), 615–622.

6 H. T. Kim, J. K. Kim, H. G. Cha, M. J. Kang, H. S. Lee, T. U. Khang, *et al.*, Biological valorization of poly(ethylene terephthalate) monomers for upcycling waste PET, *ACS Sustainable Chem. Eng.*, 2019, **7**(24), 19396–19406.

7 B. H. Shanks and P. L. Keeling, Bioprivileged molecules: creating value from biomass, *Green Chem.*, 2017, **19**(14), 3177–3185.

8 N. A. Rorrer, J. R. Dorgan, D. R. Vardon, C. R. Martinez, Y. Yang and G. T. Beckham, Renewable unsaturated polyesters from muconic acid, *ACS Sustainable Chem. Eng.*, 2016, **4**(12), 6867–6876.

9 R. M. Cywar, N. A. Rorrer, C. B. Hoyt, G. T. Beckham and E. Y. X. Chen, Bio-based polymers with performance-advantaged properties, *Nat. Rev. Mater.*, 2021, **7**(2), 83–103.

10 H. N. Lee, W. S. Shin, S. Y. Seo, S. S. Choi, J. S. Song, J. Y. Kim, *et al.*, *Corynebacterium* cell factory design and culture process optimization for muconic acid biosynthesis, *Sci. Rep.*, 2018, **8**(1), 18041.

11 G. J. Bentley, N. Narayanan, R. K. Jha, D. Salvachua, J. R. Elmore, G. L. Peabody, *et al.*, Engineering glucose metabolism for enhanced muconic acid production in *Pseudomonas putida* KT2440, *Metab. Eng.*, 2020, **59**, 64–75.

12 C. W. Johnson, D. Salvachua, P. Khanna, H. Smith, D. J. Peterson and G. T. Beckham, Enhancing muconic acid production from glucose and lignin-derived aromatic compounds via increased protocatechuate decarboxylase activity, *Metab. Eng. Commun.*, 2016, **3**, 111–119.

13 H. Zhang, B. Pereira, Z. Li and G. Stephanopoulos, Engineering *Escherichia coli* coculture systems for the production of biochemical products, *Proc. Natl. Acad. Sci. U. S. A.*, 2015, **112**(27), 8266–8271.

14 C. Ling, G. L. Peabody, D. Salvachua, Y. M. Kim, C. M. Kneucker, C. H. Calvey, *et al.*, Muconic acid production from glucose and xylose in *Pseudomonas putida* via evolution and metabolic engineering, *Nat. Commun.*, 2022, **13**(1), 4925.

15 T. Nicolai, Q. Deparis, M. R. Foulquie-Moreno and J. M. Thevelein, *In situ* muconic acid extraction reveals sugar consumption bottleneck in a xylose-utilizing *Saccharomyces cerevisiae* strain, *Microb. Cell Fact.*, 2021, **20**(1), 114.

16 I. Poblete-Castro, J. Becker, K. Dohnt, V. M. dos Santos and C. Wittmann, Industrial biotechnology of *Pseudomonas*

putida and related species, *Appl. Microbiol. Biotechnol.*, 2012, **93**(6), 2279–2290.

17 P. I. Nikel and V. de Lorenzo, *Pseudomonas putida* as a functional chassis for industrial biocatalysis: From native biochemistry to trans-metabolism, *Metab. Eng.*, 2018, **50**, 142–155.

18 K. A. Payne, M. D. White, K. Fisher, B. Khara, S. S. Bailey, D. Parker, *et al.*, New cofactor supports α,β-unsaturated acid decarboxylation via 1,3-dipolar cycloaddition, *Nature*, 2015, **522**(7557), 497–501.

19 T. Sonoki, M. Morooka, K. Sakamoto, Y. Otsuka, M. Nakamura, J. Jellison, *et al.*, Enhancement of protocatechuate decarboxylase activity for the effective production of muconate from lignin-related aromatic compounds, *J. Biotechnol.*, 2014, **192**, 71–77.

20 C. W. Johnson, D. Salvachúa, N. A. Rorrer, B. A. Black, D. R. Vardon, P. C. St. John, *et al.*, Innovative chemicals and materials from bacterial aromatic catabolic pathways, *Joule*, 2019, **3**(6), 1523–1537.

21 D. Salvachúa, P. O. Saboe, R. S. Nelson, C. Singer, I. McNamara, C. del Cerro, *et al.*, Process intensification for the biological production of the fuel precursor butyric acid from biomass, *Cell Rep. Phys. Sci.*, 2021, **2**(10), 100587.

22 X. Chen, E. Kuhn, E. W. Jennings, R. Nelson, L. Tao, M. Zhang, *et al.*, DMR (deacetylation and mechanical refining) processing of corn stover achieves high monomeric sugar concentrations (230 g L^{-1}) during enzymatic hydrolysis and high ethanol concentrations (>10% v/v) during fermentation without hydrolysate purification or concentration, *Energy Environ. Sci.*, 2016, **9**(4), 1237–1245.

23 J. R. Elmore, G. N. Dexter, D. Salvachua, M. O'Brien, D. M. Klingeman, K. Gorday, *et al.*, Engineered *Pseudomonas putida* simultaneously catabolizes five major components of corn stover lignocellulose: Glucose, xylose, arabinose, p-coumaric acid, and acetic acid, *Metab. Eng.*, 2020, **62**, 62–71.

24 Y. Zhang, T. Jiang, B. Sheng, Y. Long, C. Gao, C. Ma, *et al.*, Coexistence of two D-lactate-utilizing systems in *Pseudomonas putida* KT2440, *Environ. Microbiol. Rep.*, 2016, **8**(5), 699–707.

25 R. Davis, N. Grundl, L. Tao, M. J. Biddy, E. C. D. Tan and G. T. Beckham, *et al.*, Process design and economics for the conversion of lignocellulosic biomass to hydrocarbon fuels and coproducts: 2018 biochemical design case update: biochemical deconstruction and conversion of biomass to fuels and products via integrated biorefinery pathways, 2018.

26 R. Davis, A. Bartling and L. Tao, Biochemical conversion of lignocellulosic biomass to hydrocarbon fuels and products: 2020 state of technology and future research, 2021.

27 R. Davis, L. Tao, C. Scarlata, E. C. D. Tan, J. Ross and J. Lukas, *et al.*, Process design and economics for the conversion of lignocellulosic biomass to hydrocarbons: dilute-acid and enzymatic deconstruction of biomass to sugars and catalytic conversion of sugars to hydrocarbons, 2015.

28 D. Humbird, R. Davis, L. Tao, C. Kinchin, D. Hsu and A. Aden, *et al.*, Process design and economics for biochemical conversion of lignocellulosic biomass to ethanol. Dilute-acid pretreatment and enzymatic hydrolysis of corn stover, 2011.

29 D. R. Vardon, N. A. Rorrer, D. Salvachúa, A. E. Settle, C. W. Johnson, M. J. Menart, *et al.*, cis,cis-Muconic acid: separation and catalysis to bio-adipic acid for nylon-6,6 polymerization, *Green Chem.*, 2016, **18**(11), 3397–3413.

30 A. E. Settle, N. S. Cleveland, C. A. Farberow, D. R. Conklin, X. Huo, A. A. Dameron, *et al.*, Enhanced catalyst durability for bio-based adipic acid production by atomic layer deposition, *Joule*, 2019, **3**(9), 2219–2240.

31 G. Quintens, J. H. Vrijsen, P. Adriaensens, D. Vanderzande and T. Junkers, Muconic acid esters as bio-based acrylate mimics, *Polym. Chem.*, 2019, **10**(40), 5555–5563.

32 N. A. Rorrer, S. F. Notonier, B. C. Knott, B. A. Black, A. Singh, S. R. Nicholson, *et al.*, Production of β-ketoadipic acid from glucose in *Pseudomonas putida* KT2440 for use in performance-advantaged nylons, *Cell Rep. Phys. Sci.*, 2022, **3**(4), 100840.

33 B. Analytiq, Adipic acid price index **https://businessanalytiq.com/procurementanalytics/index/adipic-acid-price-index/2024**.

34 D. Humbird, R. Davis and J. D. McMillan, Aeration costs in stirred-tank and bubble column bioreactors, *Biochem. Eng. J.*, 2017, **127**, 161–166.

35 Argonne, Energy Systems and Infrastructure Analysis R&D GREET® Model: The Greenhouse gases, Regulated Emissions, and Energy use in Technologies Model, 2023.

36 R. A. Sheldon, The E factor at 30: a passion for pollution prevention, *Green Chem.*, 2023, **25**(5), 1704–1728.

37 E. Cavallo, M. Nobile, P. Cerrutti and M. L. Foresti, Exploring the production of citric acid with *Yarrowia lipolytica* using corn wet milling products as alternative low-cost fermentation media, *Biochem. Eng. J.*, 2020, **155**, 107463.

38 I. Khan, K. Nazir, Z. P. Wang, G. L. Liu and Z. M. Chi, Calcium malate overproduction by *Penicillium viticola* 152 using the medium containing corn steep liquor, *Appl. Microbiol. Biotechnol.*, 2014, **98**(4), 1539–1546.

39 G. Wang, B. Shi, P. Zhang, T. Zhao, H. Yin and C. Qiao, Effects of corn steep liquor on beta-poly(L-malic acid) production in *Aureobasidium melanogenum*, *AMB Express*, 2020, **10**(1), 211.

40 Y. J. Wee, J. S. Yun, D. Kim and H. W. Ryu, Batch and repeated batch production of L(+)-lactic acid by *Enterococcus faecalis* RKY1 using wood hydrolyzate and corn steep liquor, *J. Ind. Microbiol. Biotechnol.*, 2006, **33**(6), 431–435.

41 J. Dunn, N. A. F. Sather, J. Han, S. Snyder, C. He, J. Gong, D. Yue and F. You, Life-cycle analysis of Bioproducts and Their Conventional counterparts in GREET, 2015, 2015-09-01.

42 C. W. Johnson and G. T. Beckham, Aromatic catabolic pathway selection for optimal production of pyruvate and lactate from lignin, *Metab. Eng.*, 2015, **28**, 240–247.

43 D. Y. Kim, Y. B. Kim and Y. H. Rhee, Evaluation of various carbon substrates for the biosynthesis of polyhydroxyalkanoates bearing functional groups by Pseudomonas putida, *Int. J. Biol. Macromol.*, 2000, **28**, 23–29.

44 J. G. Linger, D. R. Vardon, M. T. Guarnieri, E. M. Karp, G. B. Hunsinger, M. A. Franden, *et al.*, Lignin valorization through integrated biological funneling and chemical catalysis, *Proc. Natl. Acad. Sci. U. S. A.*, 2014, **111**(33), 12013–12018.

45 A. Loeschcke and S. Thies, *Pseudomonas putida*-a versatile host for the production of natural products, *Appl. Microbiol. Biotechnol.*, 2015, **99**(15), 6197–6214.

46 J. Mi, D. Becher, P. Lubuta, S. Dany, K. Tusch, H. Schewe, M. Buchhaupt and J. Schrader, De novo production of the monoterpenoid geranic acid by metabolically engineered *Pseudomonas putida*, *Microb. Cell Fact.*, 2014, **13**, 170.

47 I. Ruhl, R. S. Nelson, R. Katahira, J. S. Kruger, X. Chen and S. J. Haugen, *et al.*, Feedstock variability impacts the bioconversion of sugar and lignin streams derived from corn stover by *Clostridium tyrobutyricum* and engineered *Pseudomonas putida*, *Microb. Biotechnol.*, 2024, DOI: 10.1111/1751-7915.70006.

48 H. Fu, L. Yu, M. Lin, J. Wang, Z. Xiu and S. T. Yang, Metabolic engineering of *Clostridium tyrobutyricum* for enhanced butyric acid production from glucose and xylose, *Metab. Eng.*, 2017, **40**, 50–58.

49 P. Zheng, J. J. Dong, Z. H. Sun, Y. Ni and L. Fang, Fermentative production of succinic acid from straw hydrolysate by *Actinobacillus succinogenes*, *Bioresour. Technol.*, 2009, **100**(8), 2425–2429.

50 Y. Ming, G. Li, Z. Shi, X. Zhao, Y. Zhao, G. Gao, *et al.*, Co-utilization of glucose and xylose for the production of poly-beta-hydroxybutyrate (PHB) by *Sphingomonas sanxanigenens* NX02, *Microb. Cell Fact.*, 2023, **22**(1), 162.

51 M. Kohlstedt, S. Starck, N. Barton, J. Stolzenberger, M. Selzer, K. Mehlmann, *et al.*, From lignin to nylon: Cascaded chemical and biochemical conversion using metabolically engineered *Pseudomonas putida*, *Metab. Eng.*, 2018, **47**, 279–293.

52 A. Ankenbauer, R. Nitschel, A. Teleki, T. Muller, L. Favilli, B. Blombach, *et al.*, Micro-aerobic production of isobutanol with engineered Pseudomonas putida, *Eng. Life Sci.*, 2021, **21**(7), 475–488.

53 A. Ankenbauer, R. A. Schafer, S. C. Viegas, V. Pobre, B. Voss, C. M. Arraiano, *et al.*, *Pseudomonas putida* KT2440 is naturally endowed to withstand industrial-scale stress conditions, *Microb. Biotechnol.*, 2020, **13**(4), 1145–1161.

54 K. H. Choi, A. Kumar and H. P. Schweizer, A 10 min method for preparation of highly electrocompetent *Pseudomonas aeruginosa* cells: application for DNA fragment transfer between chromosomes and plasmid transformation, *J. Microbiol. Methods*, 2006, **64**(3), 391–397.

55 A. Z. Werner, W. T. Cordell, C. W. Lahive, B. C. Klein, C. A. Singer, E. C. D. Tan, *et al.*, Lignin conversion to β-ketoadipic acid by Pseudomonas putida via metabolic engineering and bioprocess development, *Sci. Adv.*, 2023, **9**(36), eadj0053.

56 L. N. Jayakody, C. W. Johnson, J. M. Whitham, R. J. Giannone, B. A. Black, N. S. Cleveland, *et al.*, Thermochemical wastewater valorization via enhanced microbial toxicity tolerance, *Energy Environ. Sci.*, 2018, **11**(6), 1625–1638.

57 A. Schäfer, A. Tauch, W. Jäger, J. Kalinowski, G. Thierbach and A. Pühler, Small mobilizable multi-purpose cloning vectors derived from the *Escherichia coli* plasmids pK18 and pK19: selection of defined deletions in the chromosome of *Corynebacterium glutamicum*, *Gene*, 1994, **145**, 69–73.

58 P. Gay, D. Le Coq, M. Steinmetz, T. Berkelman and C. I. Kado, Positive selection procedure for entrapment of insertion sequence elements in Gram-negative bacteria, *J. Bacteriol.*, 1985, **164**(2), 918–921.

59 S. P. Woodworth, S. J. Haugen, W. E. Michener, K. J. Ramirez and G. T. Beckham, Muconic acid isomers and aromatic compounds analyzed by UHPLC-DAD V.2 Protocolsio, 2024.

60 H. A. Alt, A. F. Benson, S. J. Haugen, M. A. Ingraham, W. E. Michener and S. P. Woodworth, *et al.*, Analysis of sugars, small organic acids, and alcohols by HPLC-RID V.2 Protocolsio, 2024.

61 A. Sluiter, B. Hames, R. Ruiz, C. Scarlata, J. Sluiter and D. Templeton, Determination of sugars, byproducts, and degradation products in liquid fraction process samples, National Renewable Energy Laboratory, 2006, contract no.: NREL/TP-510-42623.

62 R. Frischknecht, N. Jungbluth, H.-J. Althaus, R. Hischier, G. Doka and C. Bauer, *et al.*, Implementation of Life Cycle Impact Assessment Methods. Data v2.0. Ecoinvent Report No 3; INIS-CH–10091; Ecoinvent Centre, 2007.

63 G. J. Nabuurs, R. Mrabet, A. A. Hatab, M. Bustamante, H. Clark and P. Havlík, *et al.*, Climate Change 2022: Mitigation of climate change. Contribution of working group III to the sixth assessment report of the intergovernmental panel on climate change, 2022.